

Chromosomal inversion differences correlate with range overlap in passerine birds

Daniel M. Hooper^{1*} and Trevor D. Price^{1,2}

Chromosomal inversions evolve frequently but the reasons for this remain unclear. We used cytological descriptions of 411 species of passerine birds to identify large pericentric inversion differences between species, based on the position of the centromere. Within 81 small clades comprising 284 of the species, we found 319 differences on the 9 largest autosomes combined, 56 on the Z chromosome, and 55 on the W chromosome. We also identified inversions present within 32 species. Using a new fossil-calibrated phylogeny, we examined the phylogenetic, demographic and genomic context in which these inversions have evolved. The number of inversion differences between closely related species is consistently predicted by whether the ranges of species overlap, even when time is controlled for as far as is possible. Fixation rates vary across the autosomes, but inversions are more likely to be fixed on the Z chromosome than the average autosome. Variable mutagenic input alone (estimated by chromosome size, map length, GC content or repeat density) cannot explain the differences between chromosomes in the number of inversions fixed. Together, these results support a model in which inversions increase because of their effects on recombination suppression in the face of hybridization. Other factors associated with hybridization may also contribute, including the possibility that inversions contain incompatibility alleles, making taxa less likely to collapse following secondary contact.

Chromosome inversions, a common type of chromosomal rearrangement, are regularly observed as fixed differences between species and as polymorphisms segregating within species^{1,2}. Inversions are thought to propel the evolution of sex chromosomes^{3,4}, supergene formation^{5–8}, local adaptation^{9,10} and reproductive isolation^{11–15}. Despite their evolutionary significance, the widespread presence of inversions is puzzling, as new rearrangements may be initially disfavoured due to structural underdominance in heterokaryotypes, if crossing over within the inverted region during meiosis results in the production of aneuploid gametes^{1,2,16}. Reconciling the frequency of chromosome inversions with possible selective disadvantages faced by a new inversion remains an unsolved problem.

Early models of inversion fixation considered how genetic drift might lift an underdominant inversion above 50% frequency in a local deme, after which selection favours its spread^{17–20}. This model predicts that inversion fixation rate should be independent of total population size, assuming population structure is similar across taxa^{17,20}. This was tested in the Estrildid finches (family Estrildidae) and subsequently rejected²¹, based on a strong positive relationship between the rate of inversion fixation and range size, assumed to be correlated with population size. More recent models have focused on selection mechanisms in which drift plays no part. An inversion may be adaptive and spread if its breakpoints favourably alter gene expression²², or by meiotic drive if the inversion happens to link alleles that together alter segregation distortion^{16,23}. Another set of models assumes that selective advantages of an inversion result from its effects on recombination^{24–27}. For example, recombination suppression on the Y chromosome (or W in species in which females are the heterogametic sex, such as birds) is promoted by accumulation of genes that are beneficial in the heterogametic sex but deleterious in the homogametic sex^{28,29}. Gene flow between genetically differentiated populations may also promote recombination suppressors because sets of maladaptive alleles in hybrids are eliminated as a block²⁵. In this case, genetic differences may reflect

local adaptation, genetic incompatibilities, sexually selected traits, or various combinations of these factors.

The different models that invoke selection make different predictions that can be tested with comparative analyses. All selection models depend on mutational input, which should scale with population size. However, mutational input should be particularly strongly associated with breakpoint effects and meiotic drive. This is because selective pressures resulting from these mechanisms are less dependent on environmental context and because mutations that produce favourable effects are likely to be rare. Hence, these models predict a strong scaling of inversion fixation with population size. Further, both these models are associated with an unconditional selective advantage, so any gene flow between populations or across the species barrier produced as a consequence of range overlap may remove differences between taxa. Of course, this comes with a number of caveats; for example, inversions may, by chance, capture incompatibilities and/or deleterious recessives, limiting the potential for gene flow to homogenize differences between populations. However, many recombination suppression models make the opposite prediction: that gene flow actually favours the increase of an inversion in the recipient population because the selective advantage of the inversion increases with the proportion of unfit hybrids^{25,27}. Among gene flow models, local adaptation (that is, adaptation to ecological factors) predicts associations of ecological differences between taxa with inversion increase, whereas hybridization between incompletely reproductively isolated populations favours an inversion if it captures two or more loci affecting hybrid loss of fitness, or an incompatibility locus and a mate choice locus^{24,25,27}.

Here, we consider the range size of a species to be an estimate of population size (Methods), and hence predict range size to be a relatively strong positive correlate in the breakpoint and meiotic drive models. Range overlap between closely related species indicates the potential for hybridization, essential for genetic incompatibility models. Across 32 species of Estrildid finches, both range size and

¹Committee on Evolutionary Biology, University of Chicago, Chicago, IL 60637, USA. ²Department of Ecology and Evolution, University of Chicago, Chicago, IL 60637, USA. *e-mail: dhooper1@uchicago.edu

range overlap are positively associated with the rate of inversion fixation²¹. However, range size and range overlap are themselves correlated, making it difficult to disentangle their contributions, given the sample size. Here we study 411 karyotyped bird species in order to examine the alternatives. Further, we document the widespread occurrence of inversion polymorphisms within species, and considered how the presence of these polymorphisms relates to various alternative models of inversion spread.

The Passeriformes are just 1 of 39 extant orders of birds, yet comprise over half of all avian species, with the ~6,000 species found in nearly every terrestrial habitat on the planet³⁰. The radiation has produced a large variety of ecological and morphological types: body size varies more than 350-fold between the smallest and largest species (4.2 to 1,500 g), while variation in beak shape and behaviour has produced a wide spectrum of feeding morphologies (nectarivores, granivores, insectivores, frugivores, and so on^{30,31}). In contrast, the gross structure of the passerine genome does not vary greatly, with diploid chromosome number ($2N$) falling between 76–80 for 77% of species (Supplementary Table 1)³². While chromosome fusions, fissions and translocations are apparently rare in birds, inversions are far more common^{21,32–36} (Figs. 1 and 2). Cytological evidence for the frequent occurrence of inversions in birds is corroborated by recent genomic studies that infer inversion-derived rearrangements both within and between species^{34–39}. Here we evaluate the phylogenetic, biogeographical context and genomic distribution of large pericentric inversions (that is, those encompassing the centromere) on the 9 largest autosomes and the Z chromosome (Supplementary Tables 1 and 5–8) identified from the cytological literature. We also studied the W chromosome, in which we show that movement of the centromere is particularly common. However, it is more difficult to relate centromere movement to an inversion on this chromosome, so we consider it separately.

Results

A time-calibrated phylogeny for 411 karyotyped passerine species is shown in Fig. 2 and Supplementary Figs. 1–3. The topology and divergence time estimates are congruent with a recent study that

used partially overlapping fossil sets and alternative calibration methods⁴⁰ (Supplementary Tables 4 and 5). Inversion fixation rate varies greatly across lineages (Fig. 2). To illustrate extremes, no inversions were fixed over 23.7 Myr on the lineage leading to the common iora (*Aegithina tiphia*), whereas an inversion on the sixth largest autosome separates the pied wheatear (*Oenanthe pleschanka*) from the black-eared wheatear (*O. melanoleuca*), with a divergence time of ~0.2 Myr. Thirty-two species (8%) carried chromosomal polymorphisms, and 8 of these had polymorphisms on more than one chromosome (Supplementary Table 2). This is certainly an underestimate because sample sizes were often small (Methods).

We partitioned the tree into 81 independent clades covering 284 of the 411 species, based on ecology and family membership, and evaluated roles for time, range size and range overlap, as well as various ecological variables in accounting for differences in rate of inversion accumulation (Supplementary Tables 1 and 5). Within these clades, we identified 319 autosomal pericentric inversions and 56 Z chromosome rearrangements, which gives an average rate of pericentric inversion fixation across the Z plus autosomes of 1 every 4.7 Myr of evolution. The range was from no inversions fixed over the span of 27.7 Myr (in the family Dicruridae) to 4 in 2.2 Myr (in the genus *Chloris*; Fig. 1).

In the clade analysis, range overlap (Fig. 3a) and range size (Fig. 3b) correlate with fixation rate. The best model predicting the number of inversions fixed in each clade contained just two variables: branch length and the proportion of species with overlapping ranges (median range size drops out). However, the three top models ($\Delta\text{AICc} < 2$) had similar AICc scores and model weights. Model averaged results from these top models include range size and the interaction between range size and range overlap as additional parameters, but only branch length ($P < 0.0001$) and range overlap are significant in the full average results ($P = 0.002$; Table 1 and Supplementary Table 9.1). Results were consistent regardless of whether we used a more relaxed ΔAICc cutoff to model averaging (models with $\Delta\text{AICc} < 4$) and alternative minimum range overlap cutoff values (10% or 15% pairwise range overlap) to calculate the proportion of sympatric species in each clade.

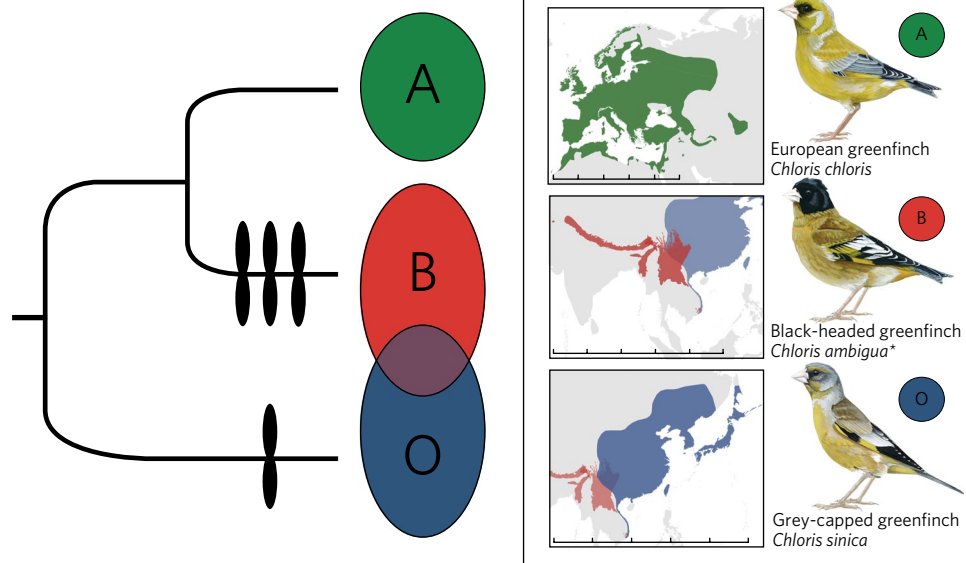


Fig. 1 | History of pericentric inversion evolution across greenfinches in the genus *Chloris*. Inversion differences are indicated by black ovals on the branches they are inferred to have fixed. Breeding ranges are coloured green, red and blue to represent the geographic distributions of *Chloris chloris*, *C. ambigua* and *C. sinica*, respectively. Scale bars depict 5,000 km distances. The three members of the black-headed greenfinch species complex (*C. ambigua*, *C. monguilloti* and *C. spinoides*) are here treated as a single species (*C. ambigua*) based on the lack of any observed premating isolation where their ranges overlap⁴³. Note that *C. chloris* and *C. sinica* actually share an inversion polymorphism on the largest autosome (Supplementary Table 1).

| Passerine families | |
|----------------------------|----------------------------|
| 1 Eurylamidae (1, 1) | 31 Pellorniidae (3, 3) |
| 2 Furnariidae (2, 2) | 32 Leiothrichidae (14, 28) |
| 3 Thamnophilidae (4, 9) | 33 Regulidae (1, 7) |
| 4 Cotingidae (1, 3) | 34 Bombycillidae (3, 0) |
| 5 Tityridae (1, 2) | 35 Sittidae (3, 6) |
| 6 Tyrannidae (14, 34) | 36 Certhiidae (1, 2) |
| 7 Aegithinidae (1, 0) | 37 Polioptilidae (1, 2) |
| 8 Tephrodornithidae (1, 2) | 38 Troglodytidae (3, 5) |
| 9 Campephagidae (3, 9) | 39 Cinclidae (1, 1) |
| 10 Oriolidae (3, 2) | 40 Mimidae (3, 6) |
| 11 Vireonidae (4, 2) | 41 Sturnidae (8, 7) |
| 12 Dicruridae (2, 0) | 42 Turdidae (20, 28) |
| 13 Monarchidae (1, 1) | 43 Muscicapidae (35, 77) |
| 14 Laniidae (8, 13) | 44 Nectariniidae (1, 2) |
| 15 Corvidae (15, 21) | 45 Chloropseidae (2, 2) |
| 16 Picathartidae (1, 4) | 46 Peucedramidae (1, 4) |
| 17 Remizidae (1, 2) | 47 Prunellidae (2, 0) |
| 18 Paridae (8, 14) | 48 Ploceidae (3, 0) |
| 19 Alaudidae (6, 9) | 49 Estrildidae (34, 83) |
| 20 Locustellidae (4, 8) | 50 Passeridae (7, 19) |
| 21 Acrocephalidae (5, 10) | 51 Motacillidae (8, 15) |
| 22 Hirundinidae (8, 13) | 52 Fringillidae (21, 40) |
| 23 Cisticolidae (2, 5) | 53 Cardinalidae (7, 5) |
| 24 Pycnonotidae (8, 11) | 54 Thraupidae (45, 52) |
| 25 Aegithalidae (3, 8) | 55 Parulidae (6, 2) |
| 26 Cettidae (1, 1) | 56 Icteriidae (1, 3) |
| 27 Phylloscopidae (9, 21) | 57 Icteridae (9, 8) |
| 28 Sylviidae (5, 10) | 58 Emberizidae (17, 55) |
| 29 Zosteropidae (5, 3) | 59 Passerellidae (22, 38) |
| 30 Timaliidae (3, 2) | |

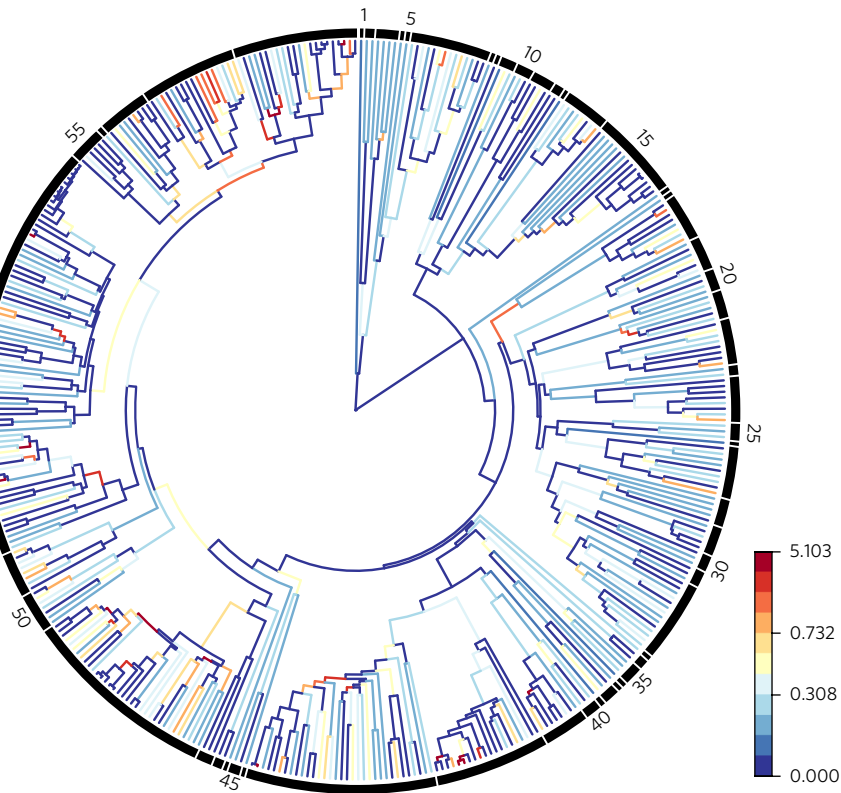


Fig. 2 | Pericentric inversion fixation rate variation on the autosomes and Z chromosome combined across the Passeriformes. Passerine families included in this study are shown on the left: numbers within parentheses refer to the number of karyotyped species and number of autosomal and Z chromosome pericentric inversions identified within each family, respectively. Families are ordered clockwise by phylogenetic position in the tree. The time-dated phylogeny for the 411 karyotyped species used in this study is shown on the right. Branches are colour-coded according to the inferred rate of pericentric inversion fixation (inversions per Myr) using the R package ggtrree⁸³ with rates partitioned according to the Jenks natural breaks method where variance within bins is minimized, while variance between bins is maximized⁸⁴.

Sister pair analyses support these findings (Fig. 3c,d). Thirty-eight sympatric sister species were significantly more likely to differ by an inversion than 9 allopatric sister pairs (two-tailed Fisher's exact test, $P = 0.045$; Fig. 3c). They also trend towards a greater number of inversion differences than allopatric sister pairs (Mann–Whitney–Wilcoxon test: $P = 0.07$; Fig. 3d). However, sympatric sister pairs are older than allopatric ones (3.9 versus 2.5 Myr to the common ancestor on average; Supplementary Fig. 4). In a comparison of general linear models, the best model explaining the presence of inversion differences between sister species contained a single parameter: whether sister species overlapped in range or not ($P = 0.047$; Table 1). Age did not contribute and no alternative models received support with $\Delta\text{AIC}_c < 2$ (Supplementary Table 9.2). Results were consistent regardless of whether we used a more relaxed ΔAIC_c cutoff to model averaging (models with $\Delta\text{AIC}_c < 4$). The sample of 12 sympatric sister species known to hybridize in nature are more often differentiated by an inversion than their 9 allopatric counterparts (although this is marginally non-significant; two-tailed Fisher exact test, $P = 0.087$; Fig. 3c), and were estimated to be of similar age (2.5 Myr for both, although hybridization may have reduced the estimate of divergence time of the sympatric species).

A major issue in the above analyses is whether branch length adequately controls for time⁴¹. Species triplets consist of a sister pair and an outgroup species, where the outgroup overlaps one of the two sisters but not the other. Comparisons of differences between the outgroup and each sister therefore test for a role of sympatry, with time completely factored out^{41,42}. Figure 1 shows a representative example where inversion differences are associated with

geographic overlap with the outgroup. This figure also indicates the only pair of allopatric sister species that differ by >2 inversions, and suggests that overlap with a third hybridizing species may have reduced the power of the previous sister pair analysis.

Results from the triplet comparison support the importance of range overlap (data in Supplementary Table 7). A conservative triplet set, where the outgroup shows no overlap with one of the two sisters, has little power ($N = 5$)—but in the three triplets that do show differences in inversion accumulation between the sisters, the species overlapping the outgroup has accumulated more inversions. In a relaxed triplet set, in which some degree of range overlap was allowed between the outgroup and both sisters, or between sisters ($N = 19$), 7 triplets showed no difference in inversion differentiation, 10 showed more inversions in the sister species that overlaps with the outgroup and 2 triplets the opposite pattern (comparing just those 12 triplets with differences, two-tailed sign rank test, $P = 0.039$). In the triplet analyses, differences in range size between sisters did not predict the number of inversion differences (regression of difference in inversion number on differences in range size, forced through the origin, $P > 0.1$).

In order to assess the possibility that mutational input strongly determines rates of inversion evolution, we studied correlates of inversion fixation rate (inversions per Myr) with chromosome size and genome content, based on assemblies from the zebra finch and collared flycatcher (Table 2). For the full 411-taxa tree, rates of inversion accumulation on the autosomes varied fourfold (Table 2). Results were qualitatively identical regardless of whether the zebra finch or collared flycatcher provided chromosome size and map distance data (Supplementary Table 10). The three top models for

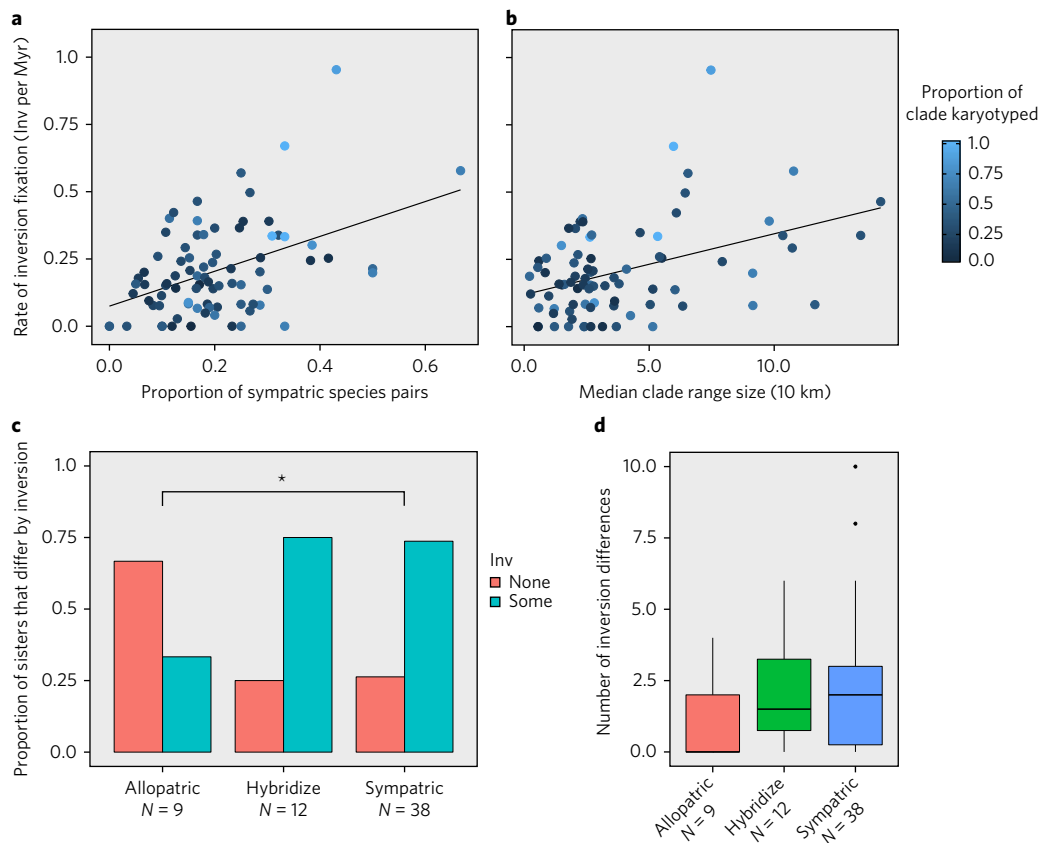


Fig. 3 | Pericentric inversion fixation rate within small clades and between sisters. **a,b**, Fixation rate across 81 clades, calculated as the total number of inversions on all chromosomes (autosomes and Z) divided by the total clade branch length summed across each chromosome (see Table 1 for statistics). Each clade is represented by a circle and shaded according to the proportion of total species with karyotype data. **c,d**, Sister species ($N = 47$) sorted into allopatric pairs, sympatric pairs (any amount of range overlap), and the subset of these sympatric sister pairs that are known to hybridize⁴³. Variation represented between sister species groups in the proportion of sister pairs with and without inversion differences (**c**), and the number of inversion differences between sister species (**d**). Boxplots (**d**) represent the number of inversion differences between sister species as the median (horizontal), the first to third quartile range (box), Q1 minus Q3 plus the interquartile range, respectively, (vertical); and outliers greater than Q3 plus 1.5 times the interquartile range (points). Statistical significance evaluated using a two-tailed Fisher's exact test, * $P < 0.05$.

the autosomes had nearly equivocal AICc scores. The full average of these models included chromosome GC content and repeat density, but neither factor was significant. Results were robust to averaging the six models with $\Delta\text{AICc} < 4$ (Supplementary Table 10). Moreover, inclusion of the Z chromosome in these analyses further reduced the fit of any mutagenic model to explain variation in inversion fixation rate between chromosomes.

Despite having fewer genes and a shorter map length than 6 of the autosomes, across the whole tree the Z chromosome

has accumulated more inversions than any autosome (Table 2). When assessed across the 81 clades, inversion fixation rate on the Z chromosome is 1.4 times greater than the average autosome (two-sample paired t -test with the 81 clades as replicates: $t_{80} = 2.1$, $P = 0.041$; Supplementary Table 8). The genomic distribution of chromosomal variants within species, which includes both polymorphisms within a population and population differences, was in roughly the same ratio: of the 32 within-species pericentric inversion variants, 6 (19%) were on the Z chromosome whereas

Table 1 | Model-averaged results for the clade and sister species analyses

| Parameter | Clades ($N=81$) | | | Sisters ($N=47$) | | |
|---------------------------------|-------------------|---------------|----------|--------------------|---------------|-------|
| | Estimate | 95% CI | P | Estimate | 95% CI | P |
| (Intercept) | 0.05 | (−1.44, 1.54) | 0.87 | −0.44 | (−2.11, 1.23) | 0.601 |
| Range overlap, arcsin | 1.57 | (0.57, 2.57) | 0.002 | 1.69 | (−0.29, 3.65) | 0.043 |
| Branch length, log Myr | 0.84 | (0.58, 1.09) | < 0.0001 | −0.001 | (−0.68, 0.68) | 0.998 |
| Range size, log km ² | 0.13 | (−0.14, 0.39) | 0.34 | 0.215 | (−0.43, 0.86) | 0.517 |
| Range overlap × range size | 0.1 | (−0.44, 0.64) | 0.72 | | | |

For clades, we used phylogenetic generalized least squares to predict the number of observed pericentric inversions. Raw correlations, ignoring phylogeny, between the number of inversions in each of the 81 clades with range overlap, range size and branch length are $r = 0.32$, $r = 0.13$ and $r = 0.53$, respectively. For sisters, we used a generalized linear model with binomial errors to predict the presence or absence of pericentric inversion differences and present the conditional model-averaged results for $\Delta\text{AICc} < 4$. Approximate 95% confidence intervals (CI) are the parameter estimate $\pm 2 \times$ standard error. P values for parameter significance were calculated by MuMIn in R⁷⁰ as the full average of the top models.

Table 2 | Genomic distribution of chromosome inversions

| Chromosome | Size (Mb) | Map length (cM) | GC content (%) | Repeat density (%) | Gene number | Branch length (Myr) | Inversions |
|------------|-----------|-----------------|----------------|--------------------|-------------|---------------------|------------|
| 1 (FAL2) | 157.4 | 320 | 39 | 0.38 | 1362 | 4449.2 | 39 |
| 2 (FAL1) | 119.8 | 245 | 39.2 | 0.23 | 1144 | 4449.2 | 71 |
| 3 (FAL3) | 115.7 | 230 | 39.4 | 0.38 | 1138 | 4449.2 | 80 |
| 4 (FAL1A) | 74.8 | 230 | 39.7 | 0.14 | 918 | 4449.2 | 108 |
| 5 (FAL4) | 70.3 | 175 | 39.2 | 0.28 | 741 | 4437.3 | 104 |
| 6 (FAL5) | 64.6 | 172 | 40.8 | 0.12 | 907 | 4398.1 | 79 |
| 7 (FAL7) | 39.3 | 125 | 41.1 | 0.14 | 518 | 4242.1 | 48 |
| 8 (FAL6) | 37.2 | 122 | 41.6 | 0.19 | 528 | 4088.8 | 35 |
| 9 (FAL8) | 32 | 95 | 41.3 | 0.5 | 425 | 3973.8 | 23 |
| Z | 59.7* | 165 | 39.2 | 1.5 | 712 | 4449.2 | 121 |

Autosomes are listed in order of descending size with their presumed homology to the collared flycatcher (*Ficedula albicollis*) genome given in parentheses. Values for chromosome size and map length come from the collared flycatcher genome³⁷ while GC content, repeat density and gene number come from the zebra finch (*Taeniopygia guttata*) genome^{36–38}. Variation in branch lengths by chromosome reflects species with missing data. *Zebra finch Z chromosome is 72.9 Mb in length.

10% would be naively expected, given we compared them with 9 autosomes.

We have separated the W chromosome from the main analyses because the genomic make-up of the W chromosome (notably large expanses of repetitive DNA) means that centromere movement may be related less clearly to inversions than on the other chromosomes. Further, a large fraction of the W chromosome is non-recombining, implying that inversions within that region would have no effect on recombination. Despite this, the W showed more centromeric movement than the Z when comparing across clades (Supplementary Table 5, paired *t*-test: $t_{74} = 2.5$, $P = 0.013$) and its rate of evolution was 2.4 times that of the average autosome ($t_{74} = 4.1$, $P = 0.0001$). Within species, polymorphisms are also common on the W chromosome (11 observed, compared with an average of 3.2 polymorphisms per chromosome for the Z and 9 autosomes; Supplementary Table 2).

Discussion

Inversions in birds are common. Large pericentric inversions regularly separate even closely related species (Fig. 1). We have restricted our analyses to only those pericentric inversions large enough to be detectable via cytological analysis, which excludes not only all paracentric inversions but also small pericentric inversions, so these counts are surely an underestimate of the true extent of chromosome inversion variation in passerines, as is becoming increasingly clear from genomic studies^{34–39}. Large pericentric inversion polymorphisms within species are also common and clearly underestimated in this study, as sample sizes were often small. Indeed, twice as many individuals were karyotyped in the 31 passerine species found to have inversions segregating versus the study as a whole (9.9 versus 4.8 individuals, respectively; excluding 3 species of large sample size, Supplementary Fig. 5; Supplementary Table 2).

The main result is that the strongest correlate of inversion fixation after accounting for time is range overlap, not range size. Range overlap is pertinent to models of inversion spread because it gives the possibility for hybridization between taxa. F1 hybrids should more rarely recombine parental allelic combinations in the inverted region compared to co-linear chromosomes, with the consequence that fewer backcrosses carry deleterious combinations—whether these deleterious consequences are for ecological reasons, or because of genetic incompatibilities^{25,27}. Secondary contact between long divergent forms is regularly associated with hybridization and genetic exchange^{43,44}. We know for birds that hybrid zones regularly form between taxa that can be millions of years old⁴⁵ (Supplementary Table 6), and the generation of complete infertility of hybrids takes a comparable length of time⁴⁶. Together, the evidence suggests that

one contribution to the establishment of pericentric inversions in passerines stems from their selective advantage in keeping sets of adapted alleles together. We first consider caveats before returning to the main results.

A major issue is that allopatric sister species may exhibit fewer inversion differences than sympatric sisters due to a lower mutational input, either because they have smaller population sizes or because they are younger. In fact, sympatric sister pairs are of similar range size to allopatric pairs and, statistically, our evidence suggests that range size is of secondary importance as a contributor to inversion fixation. However, sympatric sister pairs are older than allopatric ones, and age differences do correlate with the number of inversions fixed. Nevertheless, all our tests indicate that this is unlikely to completely eliminate a role for range overlap. Two examples illustrate the case for an association between range overlap and inversion fixation. First, tits in the genera *Periparus* and *Pardaliparus* last shared a common ancestor 7 Ma (5.2–8.9 Ma, 95% highest posterior density, HPD), have largely allopatric distributions (no pair of species overlap in range more than 20%), and have no known inversion differences. In stark contrast, an Asian clade of tits in the genus *Poecile* diverged 4.3 Ma (3.1–5.6 Ma, 95% HPD), are largely sympatric (two-thirds of pairs), and the species examined differ by up to seven pericentric inversions (Supplementary Table 5). A second example comes from greenfinches in the genus *Chloris* (family Fringillidae; Fig. 1). Inversion differentiation between *C. sinica* and sympatric *C. ambigua* has outpaced inversion differentiation between *C. sinica* and allopatric *C. chloris*. In both the tits and the greenfinches, a model where gene flow promotes the spread of inversions has additional support because hybridization between overlapping species has been recorded in nature (in the tits, between *Poecile montanus* and *P. palustris*, and in the finches, between *C. ambigua* and *C. sinica*)⁴³.

The second issue is whether hybridization promotes inversion fixation or instead incompatibilities associated with inversions prevent sympatric species collapse. In the latter case, species that overlap in range may show more inversions than allopatric ones because those allopatric forms without inversions are more likely to fuse following secondary contact^{11,12}. However, this still raises the issue of what forces cause inversions to arise in allopatry, and why they should differentially accumulate incompatibilities. In a previous model⁴⁷, inversions accumulate incompatibilities because they trap alleles that would otherwise flow across the species border. Therefore, it may be that inversion promotion and inversion preservation are best considered as complementary explanations, both being integrally tied to recombination suppression in the face of gene flow.

Further separating the promotion or preservation models is difficult. For example, the relatively large number of inversions on the Z (and possibly on the W) may reflect Haldane's rule processes and inversion preservation, because they cut off gene flow through the heterogametic sex early (notably because of recessive incompatibilities exposed in the heterogametic sex, and Z-W interactions^{33,48}). But these same processes may select for inversions to increase on the sex chromosomes because they tie together those incompatibilities that are most strongly expressed in young species pairs where hybridization produces at least some fertile F1 offspring. It has been noted that under a model of differential merging, young sympatric pairs should form a subset of all allopatric pairs⁴⁹, which implies that some allopatric pairs should differ in inversions. In our study, most young allopatric sisters do not differ in inversions (Supplementary Fig. 4). This would appear to support a role for secondary contact in promoting their spread. However, sample size is small (9 pairs of allopatric sisters) and 1 pair of allopatric sisters does differ by 4 inversions (3 fixed differences and an inversion polymorphism). This 4-inversion allopatric pair may therefore be consistent with the idea of preservation on contact, but that particular example can be explained away because the outgroup to the sisters hybridizes with the species that has accumulated 3 of the inversions (Fig. 1).

Other processes beyond those associated with recombination suppression surely contribute to inversion accumulation. If gene flow is a frequent event following establishment in sympatry, and breakpoint selection or meiotic drive has driven accumulation of inversions in allopatry, we have argued that inversions would introgress across the species barrier rather than contribute to species differences. We also suggested that these models predict a particularly strong scaling with population size because they depend on mutagenic input. However, these predictions assume that many other factors are held constant. For example, large inversions capture multiple alleles, possibly including rare deleterious recessives, which would prevent fixation of the inversion despite whatever selective forces favour its increase²⁵. Further, the rapid movement of the centromere on the W chromosome is most easily explained by high mutagenic input (Methods). If any of these centromere movements are a consequence of inversions, they are unlikely to be due to recombination suppression, because recombination is already limited to a small pseudo-autosomal region on the W³⁸. The Z chromosome has a higher inversion fixation rate than any autosome, which may reflect an elevated mutagenic input due to a male-biased mutation rate, as the Z chromosome spends two-thirds of its time in males. However, as noted above, the Z may be particularly likely to accumulate inversions as a consequence of their effects on recombination suppression in hybrid zones, as well as in cases of sexual conflict.

Processes that depend strongly on mutagenic input can also be evaluated using information on genome content (Table 2). The distribution of chromosome inversions detected using comparative genomic approaches in birds is positively associated with chromosome size^{36,37} and inversion breakpoints are often located in regions with elevated recombination rates, GC content and repeat density³⁷. These results suggest a role for models where mutagenic input is the rate-limiting factor, such as the breakpoint and meiotic drive models. However, these results were not replicated here, and we found few correlates of genome content with inversion accumulation (although repeat density is suggestive.) A primary reason for the difference between the genomic studies and ours probably resides in the different size classes of inversions considered between studies²¹. Inversions detected from comparing whole-genome alignments³⁶ or high-resolution linkage maps³⁷ are capable of finding structural variants orders of magnitude smaller than the exclusively large inversions we identified from cytological data. We suggest that the large pericentric inversions considered here may become established in a different manner to small rearrangements, because they

are potentially associated with both higher fitness costs and greater selective advantages than the more comprehensive set of inversions found in comparative genomic surveys.

In conclusion, our results generally support recombination suppression mechanisms as one cause of inversion differences between species. The presence of many within-species inversion polymorphisms in birds implies that other mechanisms contribute to inversion accumulation beyond those driven by range overlap, but many of these mechanisms may also involve recombination suppression. For example, female preferences for male traits are more likely to increase if the trait and preference are in strong linkage disequilibrium⁵⁰. Whatever the selective advantage, if favoured inversions capture deleterious alleles when they first arise, they may not increase to fixation and result in stable polymorphisms²⁵, as inferred for at least two bird species^{6–8}. Two examples are known of the same inversion polymorphisms segregating in more than one species (Supplementary Table 2), which may reflect introgression or preservation through the speciation event. Whether inversion polymorphisms have arisen by a different class of mechanisms than inversions fixed between species remains to be determined.

Methods

Identifying inversions. We identified chromosome inversions from classic studies of gross karyotype structure that encompass nearly 8% of all passerine species and >50% of passerine families. Of the 428 passerine species that have had their karyotypes described, we discarded 15 because the cytological data was not of sufficiently high quality to include in this study and 2 because no suitable genetic data currently exists for them and no tissue materials were available. We analysed cytological data for the remaining 411 species, representing birds from 59 families (Supplementary Table 1). Data was sourced from 111 studies that span five decades of cytological research. Methods used to describe karyotype varied from simple Giemsa staining to fluorescent *in situ* hybridization with chromosome painting. Sampling rigor varied across studies with respect to the number (with an average of 7 karyotyped individuals per taxon, range from 1 to 432; Supplementary Fig. 5) and sex representation of each species (data from both males and females in 296 of 411 species). Sampling information was not given for 29 species. Due to the considerable heterogeneity in the quality and quantity of karyotype descriptions between species and studies, we focus on a simple yet powerful trait with which to infer pericentric chromosome inversion differences between and within species: centromere position.

For each species, we converted centromere position for the 9 largest autosomal chromosomes and both sex chromosomes into character state data (Supplementary Table 1). We scored each chromosome for approximate centromere position (that is, whether it was metacentric, sub-metacentric, sub-telocentric or telocentric), following conventions established previously⁵¹. We identified homologous chromosomes between species based on their physical size, shared banding pattern, and matching chromosome painting as the information was available. When assignment of chromosome homology was not absolute, for instance due to a lack of banding information for similarly sized chromosomes, we conservatively assigned homology in a way that would not result in centromere movement. This was most common for the second and third as well as the fourth and fifth largest autosomal chromosomes, which are of similar sizes (Table 2). However, we treated the centromere position of a chromosome as distinct when species shared the same general classification (for example, if both were sub-metacentric) but the authors (of the studies from which we collected the banding information) noted that the banding pattern flanking the centromere consistently differed. We only include pericentric inversions in our analyses as the cytological data has far less power to identify paracentric inversions (those not encompassing the centromere). Centromere repositioning can result from processes other than pericentric inversion, such as the expansion of transposable elements, the redistribution of heterochromatin^{52–54}, and the evolution of neo-centromeres^{55,56}. We found no evidence, however, of these alternative mechanisms of centromere repositioning in the 85 species with banding data available, as centromere movement was supported by inversion of proximal banding patterns. While we recorded centromere position for the W chromosome for all taxa with females karyotyped, results from this chromosome were analysed independently in all further analyses as centromere movement on the W chromosome appears to be particularly labile and may be more likely to result from processes other than chromosome inversion^{54,56}.

While the distribution of fixed inversion differences can be used to infer historical patterns of selection, the mechanisms of selection affecting inversions are best studied when rearrangements still segregate in natural populations. We therefore evaluated all species for the occurrence of pericentric inversion polymorphisms and for the presence of inversions present in different parts of species ranges (Supplementary Tables 1 and 2). Polymorphisms segregating within populations were often noted in the paper of interest, but the majority

of geographic variants are first reported in this study, as they generally depend on comparing different published studies (Supplementary Table 2). Of the 50 total rearrangement polymorphisms identified, two are likely to be a product of chromosome translocation and three are shared between species —two across three species and one between two species (Supplementary Table 2).

Phylogenetic analysis. To characterize the phylogenetic distribution of chromosome inversion fixation, we built a time-dated phylogeny for the 411 passerine species under study. We gathered sequence data from six genes: two mitochondrial: *cytb* and *ND2*; and four nuclear: myoglobin (*MG*) exons 2–3, ornithine decarboxylase (*ODC*) exons 6–8, β -fibrinogen (*FIB5*) exons 5–6, and recombination activating protein-1 (*RAG1*). Data were primarily sourced from GenBank. For 12 karyotyped species with no or low sequence representation, we generated the sequences ourselves using standard methods (Supplementary Table 3). Phylogenetic and dating analyses were conducted using BEAST v1.8.2⁵⁷. Sequence data was partitioned by locus, each with its own uncorrelated lognormal relaxed clock, and assigned the optimal-fit model of sequence evolution estimated for each locus using jModelTest v0.1.1⁵⁸. The phylogeny was time-calibrated using 20 fossil calibrations broadly dispersed both in time and topology (Supplementary Fig. 1 and Table 2). This is the most extensive fossil calibration effort to date within the Passeriformes. Each fossil calibration was applied to its corresponding node as a minimum age bound using a conservative uniform prior based on the age of the fossil itself and 80 Ma. We ran BEAST for 50 million generations and sampled every 5,000 for a total of 10,000 trees of which the first 1,000 were discarded as burn-in. We assessed run length and appropriate sampling for each parameter using Tracer v1.6⁵⁷. Using TreeAnnotator v1.7.2⁵⁷, we extracted the maximum clade credibility tree, with associated confidence intervals for median node heights (Fig. 2 and Supplementary Fig. 2).

Phylogenetic distribution of inversion fixation. To map inversion evolution across the phylogeny, we estimated the ancestral centromere position (up to 4 possible states: metacentric, sub-metacentric, sub-telocentric or telocentric) for each chromosome at each node in the tree by maximum likelihood in Mesquite v2.7.5⁵⁹ (which produces a joint reconstruction of all nodes across the whole tree). We obtained the maximum likelihood estimate for each ancestral centromere position for each chromosome at every node. Inversions were inferred to have occurred on branches where the karyotype of an internal node differed from subsequent nodes or the tips and was supported by a maximum likelihood, $P > 0.75$. We used this phylogenetic representation of inversion evolution in passerines to investigate the drivers of inversion fixation between species and within the genome. We conducted analyses at two different phylogenetic levels. First, we defined 81 clades in total comprising between 3 and 85 species and, second, we used 47 sister species pairs.

Chromosome inversion differences between clades. We partitioned the phylogeny of karyotyped taxa into 81 clades of closely related species to examine the factors associated with broad scale variation in chromosome inversion evolution. Many clades contain additional species that were not karyotyped, and hence not included in the tree, yet these species may influence chromosomal evolution in the focal taxa; for example, through range overlap. To take this into account, we used phylogenies from 55 published family-level studies to determine which non-karyotyped species to include in clade-level analyses (Supplementary Table 5). Clades were assigned based on the following grouping criteria: the two most distantly related karyotyped species were less than 15 Myr diverged, member species were the result of speciation within a single geographic region (that is, all clade members speciated in Australia), member species were ecologically similar (granivores, insectivores, frugivores, nectarivores or omnivores), a comprehensive family-level phylogeny exists to identify non-karyotyped member taxa, and they encompassed at least three species including non-karyotyped taxa. After filtering based on the above criteria, 284 of 411 karyotyped species were assigned to 81 clades (Supplementary Tables 1 and 5).

We measured variation in karyotype evolution across passerine clades by counting the total number of inversions that had fixed on each chromosome, summing over all branches within the clade. We did not include inversion polymorphisms in this count unless the ancestral conformation of the chromosome polymorphic for an inversion, determined in Mesquite, was neither of the segregating forms. We calculated clade branch length as the sum of branch lengths for species with centromere position scored at each of the 9 autosomes and the Z chromosome. For example, if all species within a clade had complete karyotype records (that is, centromere position scored for all 10 chromosomes), the branch length value of that clade was the sum of all branches multiplied by a factor of 10. For species missing data for a chromosome, the length of the branch leading to that species was removed from the clade total according to the total number of missing chromosomes (that is, if a species was missing data at two chromosomes, then 2 times the branch length to that species was subtracted from the clade total).

We collected range overlap, range size, and body mass data from the complete taxon set for each clade (that is, including both karyotyped and non-karyotyped species) in order to evaluate the extent to which variation in demography (population size) and speciation history (range overlap) has impacted inversion

evolution (Supplementary Table 5). We extracted range data for all species from natureserve.org using the programs Sp⁶⁰ and PBSmapping in R⁶¹. We assigned each clade a range size value corresponding to the median range size (km^2) of all member taxa. Median body mass (g) for each clade was calculated from published data⁶². We used range size together with body mass in mixed models as proxies for population size based on the positive relationship between the geographic area a species occupies and its nucleotide diversity^{63–65} and the negative relationship generally observed between body size and population density⁶⁶. We assigned a range overlap score to each clade based on the proportion of all species whose ranges overlap others by >20% (range overlap is the fraction of the range of species A that overlaps that of species B, which typically differs from the fraction of the range of species B that overlaps with that of species A). We also scored all species known to hybridize in the wild⁴³. We include hybridizing taxa together with taxa whose ranges are sympatric because both imply there is at least the potential for gene flow between taxa. Lastly, we considered a broad role for ecology on chromosome inversion evolution across clades according to the feeding guild used when defining clades (that is, clades defined as comprising granivores, insectivores, frugivores or omnivores³⁰).

The total number of inversions, branch length, range size, and body mass were log transformed, range overlap was arcsine square root transformed, and all variables were centered before analysis⁶⁷. We then evaluated the extent to which the number of inversions that had fixed in each clade was associated with branch length, range overlap, range size, body mass and ecology using generalized least squares to take into account phylogenetic relationships⁶⁸. To do this, we used the NLME package in R⁶⁹, with the expected error covariance matrix computed based on the phylogenetic distances between clades (Supplementary Fig. 3). To assess the relative importance of each factor on the number of inversions fixed in each clade, we compared all possible models and selected the best-fit model based on sample size-corrected information criteria (AICc) using the R package MuMin⁷⁰.

Chromosome inversion differences between sister species. We considered the distribution of inversions between sister species, including both fixed differences and inversions segregating in one taxon but not the other. We determined which karyotyped species pairs were true sisters using the available phylogenetic literature (Supplementary Table 6). We considered a sister pair to hybridize if they had documented hybrid zones or extensive natural hybridization where they co-occur⁴³. In total, we identified 47 true sisters with both species karyotyped.

For all 47 sister pairs, we calculated the number of inversion differences between them, combined branch length (that is, twice their time to common ancestry), average range size, range overlap, and whether they are known to hybridize in the wild (12 of 47 pairs are known to do so). Inversion difference was scored both as a binary character (no inversions or at least one inversion difference) and as a count (total number of inversion differences). Range overlap was evaluated as a binary character: no overlap or some overlap. We only used this binary categorization because subdividing sisters who overlapped in range into either parapatric (average overlaps of the two species <20%) or sympatric (>20% overlap) bins did not improve the fit of any model or alter the results in any way. We used a linear model to examine the interaction between the number of sister pair inversion differences and each factor (age, range size, range overlap and hybridization) after transforming the continuous character data as described for analysis of clades. Lastly, we assessed whether sister species with overlapping ranges, and the subset of sympatric sisters known to hybridize, are more likely to differ by an inversion than allopatric sisters using a Fisher's exact test.

Triplets. Genetic distance is not time but rather an estimate of time, and one that can come with substantial error⁴¹. This error can diminish the true contribution of time and elevate the importance of alternative factors⁴¹. A method to completely control for the potentially confounding influence of time is the use of species triplets^{42,71}. A triplet consists of a sister species pair (A and B) and a single outgroup taxon (O). Both sister taxa have by definition been separated from the outgroup for the same length of time. If O overlaps B but not A, then the presence of more inversion differences between O and B than O and A gives support for a role of range overlap independent of time (Fig. 1). We assembled a set of species triplets from the phylogeny of karyotyped species and published phylogenies, using the following criteria: both sister species A and B have been karyotyped, A and B are allopatric, and B overlaps in range with O but species A does not. This resulted in just 5 triplets (Supplementary Table 7). We relaxed the criteria to allow: (1) range overlap between A and B, and (2) range overlap between A and O as long as they were not sympatric (that is, ranges overlapped less than 20%) and overlapped in range less than B and O. The average extent of range overlap between species A and O, when they did overlap, was 3 times less than the extent of range overlap between B and O. Nineteen triplets were present after applying the relaxed filtering criteria.

We counted the number of inversions inferred to have occurred along the branches leading to species A and B, respectively, based on the distribution of fixed inversions in the complete karyotyped species phylogeny. We also included inversion polymorphisms found in one but not the other taxon. We scored each triplet as follows: more inversions in A than B, more inversions in B than A, or no difference in the number of inversions between A and B. We evaluated the direction and significance of the relationship between range overlap and inversion

evolution across all triplets by applying a signed rank test to those sisters where the number of inversions differed.

Genomic distribution of chromosome inversions. Inversion fixation models that depend heavily on mutational input (for example, meiotic drive and breakpoint selection) predict a strong correlation with range size but they also predict a strong association with mutation rate. In a final analysis to examine the extent to which inversion evolution is a mutation limited process, we examined the distribution of chromosome inversions across the genome and evaluated the degree to which the number of inversions fixed on a chromosome (Supplementary Table 8) was associated with four possible mutagenic processes. First, if the mutation rate for inversions is constant per DNA base, the number of inversions should be proportional to chromosome size. Second, because inversions are derived from double-stranded meiotic breaks, the number of inversions on a chromosome could best be predicted by its map length or GC content — features associated with the number of cross-overs per chromosome^{72,73}. Third, as inversion breakpoints are often located in repeat-rich regions of chromosomes^{35–37}, we tested for an association between the number of inversions and a chromosome's repeat density. Fourth, we asked if the dynamics of inversion fixation on the sex chromosomes and the autosomes differ²¹. Mutation rates on the Z chromosome should be relatively high in birds because the Z spends two-thirds of the time in males, however this mutational advantage needs to overcome the fact that there are only three-quarters as many copies of the Z as each of the autosomes^{36,74,75}.

Primary estimates of chromosome physical size, map length, and GC content were derived from the collared flycatcher genome assembly and linkage map³⁷ and chromosome repeat density was estimated from a RepeatMasker annotation of the zebra finch genome (<http://www.repeatmasker.org>⁷⁶). We use chromosome size and map length data from the collared flycatcher but obtained identical results when analyses were repeated using chromosome size and map distance data derived from zebra finch^{77,78} and hooded crow (*Corvus cornix*⁷⁹; Supplementary Table 10). Comparative genomic studies indicate that chromosome size, GC content, and repeat density are conserved even between species in different avian orders^{36,37,56}. While the recombination landscape may have phylogenetic signal^{80–82}, recombination hotspots are well maintained in passerines studied so far³⁸.

We used data from all 411 karyotyped species to examine the correlation between chromosome inversion fixation rate and chromosome physical size, GC content, repeat density, and map length, using each chromosome as a replicate. To account for species with missing data, we use inversion fixation rate (total number of inversions fixed on a chromosome divided by the combined branch length for all species with data for that chromosome) rather than inversion number (Supplementary Table 8). Independent variables were log-transformed. We evaluated support for alternative mutagenic hypotheses by comparing between all possible linear models and selected the best-fit model using the R package MuMIn⁸⁰. Restricting the analysis to the 291 species with complete karyotype data (that is, documented centromere position for all 10 chromosomes) yielded a similar result (Supplementary Table 10). Finally, we tested for significant differences in the rate of inversion fixation between the autosomes and the Z chromosome using the 81 independent passerine clades defined above as replicates and paired *t*-tests.

Data availability. All cytological and demographic data collected and/or analysed during this study are included in this published article (and its Supplementary Information files). All genetic data generated during this study are available on GenBank (accession numbers: MF458370 to MF458470).

Received: 27 March 2017; Accepted: 19 July 2017;

Published online: 28 August 2017

References

- Hoffmann, A. A. & Rieseberg, L. H. Revisiting the impact of inversions in evolution: from population genetic markers to drivers of adaptive shifts and speciation? *Annu. Rev. Ecol. Syst.* **39**, 21–42 (2008).
- Faria, R. & Navarro, A. Chromosomal speciation revisited: rearranging theory with pieces of evidence. *Trends Ecol. Evol.* **25**, 660–669 (2010).
- Wilson, M. A. & Makova, K. D. Genomic analyses of sex chromosome evolution. *Annu. Rev. Genom. Hum. Genet.* **10**, 333–354 (2009).
- Wright, A. E., Harrison, P. W., Montgomery, S. H., Pointer, M. A. & Mank, J. E. Independent stratum formation on the avian sex chromosomes reveals inter-chromosomal gene conversion and predominance of purifying selection on the W chromosome. *Evolution* **68**, 3281–3295 (2014).
- Kunte, K. et al. Doublesex is a mimicry supergene. *Nature* **507**, 229–232 (2014).
- Küpper, C. et al. A supergene determines highly divergent male reproductive morphs in the ruff. *Nat. Genet.* **48**, 79–83 (2015).
- Lamichhaney, S. et al. Structural genomic changes underlie alternative reproductive strategies in the ruff (*Philomachus pugnax*). *Nat. Genet.* **48**, 84–88 (2016).
- Tuttle, E. M. et al. Divergence and functional degradation of a sex chromosome-like supergene. *Curr. Biol.* **26**, 344–350 (2016).
- Lowry, D. B. & Willis, J. H. A widespread chromosomal inversion polymorphism contributes to a major life-history transition, local adaptation, and reproductive isolation. *PLoS Biol.* **8**, e1000500 (2010).
- Jones, F. C. et al. The genomic basis of adaptive evolution in threespine sticklebacks. *Nature* **484**, 55–61 (2012).
- Rieseberg, L. H. Chromosomal rearrangements and speciation. *Trends Ecol. Evol.* **16**, 351–358 (2001).
- Noor, M. A., Grams, K. L., Bertucci, L. A. & Reiland, J. Chromosomal inversions and the reproductive isolation of species. *Proc. Natl Acad. Sci. USA* **98**, 12084–12088 (2001).
- Brown, K. M., Burk, L. M., Henagan, L. M. & Noor, M. A. F. A test of the chromosomal rearrangement model of speciation in *Drosophila pseudoobscura*. *Evolution* **58**, 1856–1860 (2004).
- Ayala, D., Guerrero, R. F. & Kirkpatrick, M. Reproductive isolation and local adaptation quantified for a chromosome inversion in a malaria mosquito. *Evolution* **67**, 946–958 (2012).
- Fishman, L., Stathos, A., Beardsley, P. M., Williams, C. F. & Hill, J. P. Chromosomal rearrangements and the genetics of reproductive barriers in *Mimulus* (monkey flowers). *Evolution* **67**, 2547–2560 (2013).
- King, M. *Species Evolution: The Role Of Chromosome Change* (Cambridge Univ. Press, Cambridge, 1993).
- Lande, R. Effective deme sizes during long-term evolution estimated from rates of chromosomal rearrangement. *Evolution* **33**, 234–251 (1979).
- Hedrick, P. W. The establishment of chromosomal variants. *Evolution* **35**, 322–332 (1981).
- Walsh, J. B. Rate of accumulation of reproductive isolation by chromosomal rearrangements. *Am. Nat.* **120**, 510–532 (1982).
- Lande, R. The fixation of chromosomal rearrangements in a subdivided population with local extinction and colonization. *Heredity* **54**, 323–332 (1985).
- Hooper, D. M. & Price, T. D. Rates of karyotypic evolution in Estrildid finches differ between island and continental clades. *Evolution* **69**, 890–903 (2015).
- Puig, M., Caceres, M. & Ruiz, A. Silencing of a gene adjacent to the breakpoint of a widespread *Drosophila* inversion by a transposon-induced antisense RNA. *Proc. Natl Acad. Sci. USA* **101**, 9013–9018 (2004).
- White, M. Chain processes in chromosomal speciation. *System. Zool.* **27**, 285–298 (1978).
- Charlesworth, D. & Charlesworth, B. Selection on recombination in clines. *Genetics* **91**, 581–589 (1979).
- Kirkpatrick, M. & Barton, N. H. Chromosome inversions, local adaptation, and speciation. *Genetics* **173**, 419–434 (2006).
- Feder, J. L., Gejji, R., Powell, T. H. Q. & Nosil, P. Adaptive chromosomal divergence driven by mixed geographic mode of evolution. *Evolution* **65**, 2157–2170 (2011).
- Dagilis, A. J. & Kirkpatrick, M. Prezygotic isolation, mating preferences, and the evolution of chromosomal inversions. *Evolution* **70**, 1465–1472 (2016).
- Ohno, S. *Sex Chromosomes And Sex-Linked Genes* (Springer, Berlin, Heidelberg, 1967).
- Charlesworth, B. The evolution of sex chromosomes. *Science* **251**, 1030–1033 (1991).
- Del Hoyo, J., Elliott, A. & Christie, A. D. *Handbook of the Birds of the World* Vols 8–16 (Lynx Edicions, Barcelona, 2003–2011).
- Price, T. D. et al. Niche filling slows the diversification of Himalayan songbirds. *Nature* **509**, 222–225 (2014).
- Christidis, L. *Animal Cytogenetics 4: Chordata 3 B: Aves* (Gebrüder Borntraeger, Stuttgart, 1990).
- Price, T. *Speciation in Birds* (Roberts, Greenwood Village, Colorado, 2008).
- Aslam, M. L. et al. A SNP based linkage map of the turkey genome reveals multiple intrachromosomal rearrangements between the turkey and chicken genomes. *BMC Genomics* **11**, 647 (2010).
- Skinner, B. M. & Griffin, D. K. Intrachromosomal rearrangements in avian genome evolution: evidence for regions prone to breakpoints. *Heredity* **108**, 37–41 (2011).
- Zhang, G. et al. Comparative genomics reveals insights into avian genome evolution and adaptation. *Science* **346**, 1311–1320 (2014).
- Kawakami, T. et al. A high-density linkage map enables a second-generation collared flycatcher genome assembly and reveals the patterns of avian recombination rate variation and chromosomal evolution. *Mol. Ecol.* **23**, 4035–4058 (2014).
- Singhal, S. et al. Stable recombination hotspots in birds. *Science* **350**, 928–932 (2015).
- Knief, U. et al. Fitness consequences of polymorphic inversions in the zebra finch genome. *Genome Biol.* **17**, 199 (2016).
- Claramunt, S. & Cracraft, J. A new time tree reveals Earth history's imprint on the evolution of modern birds. *Sci. Adv.* **1**, e1501005 (2015).

41. Hudson, E. J. & Price, T. D. Pervasive reinforcement and the role of sexual selection in biological speciation. *J. Hered.* **105**, 821–833 (2014).
42. Noor, M. A. F. How often does sympatry affect sexual isolation in *Drosophila*? *Am. Nat.* **149**, 1156–1163 (1997).
43. McCarthy, E. M. *Handbook of Avian Hybrids of the World* (Oxford Univ. Press, Oxford, 2006).
44. Payseur, B. A. & Rieseberg, L. H. A genomic perspective on hybridization and speciation. *Mol. Ecol.* **25**, 2337–2360 (2016).
45. Weir, J. T. & Price, T. D. Limits to speciation inferred from times to secondary sympatry and ages of hybridizing species along a latitudinal gradient. *Am. Nat.* **177**, 462–469 (2011).
46. Price, T. D. & Bouvier, M. M. The evolution of F1 postzygotic incompatibilities in birds. *Evolution* **56**, 2083–2089 (2002).
47. Navarro, A. & Barton, N. H. Accumulating postzygotic isolation genes in parapatry: a new twist on chromosomal speciation. *Evolution* **57**, 447–459 (2003).
48. Turelli, M. & Orr, H. A. Dominance, epistasis and the genetics of postzygotic isolation. *Genetics* **154**, 1663–1679 (2000).
49. Coyne, J. A. & Orr, H. A. Patterns of speciation in *Drosophila*. *Evolution* **43**, 362–381 (1989).
50. Lande, R. Models of speciation by sexual selection on polygenic traits. *Proc. Natl Acad. Sci. USA* **78**, 3721–3725 (1981).
51. Levan, A., Fredga, K. & Sandberg, A. A. Nomenclature for centromeric position on chromosomes. *Hereditas* **52**, 201–220 (1964).
52. Krasikova, A., Daks, A., Zlotina, A. & Gaginskaya, E. Polymorphic heterochromatic segments in Japanese quail microchromosomes. *Cytogenet. Genome Res.* **126**, 148–155 (2009).
53. Zlotina, A. et al. Centromere positions in chicken and Japanese quail chromosomes: *de novo* centromere formation versus pericentric inversions. *Chromosome Res.* **20**, 1017–1032 (2012).
54. Rutkowska, J., Lagisz, M. & Nakagawa, S. The long and the short of avian W chromosomes: no evidence for gradual W shortening. *Biol. Lett.* **8**, 636–638 (2012).
55. Marshall, O. J., Chueh, A. C., Wong, L. H. & Choo, K. H. A. Neocentromeres: new insights into centromere structure, disease development, and karyotype evolution. *Am. J. Hum. Genet.* **82**, 261–282 (2008).
56. Ellegren, H. The evolutionary genomics of birds. *Annu. Rev. Ecol. Evol. Syst.* **44**, 239–259 (2013).
57. Drummond, A. J., Suchard, M. A., Xie, D. & Rambaut, A. Bayesian phylogenetics with BEAUTi and the BEAST 1.7. *Mol. Biol. Evol.* **29**, 1969–1973 (2012).
58. Posada, D. jModelTest: phylogenetic model averaging. *Mol. Biol. Evol.* **25**, 1253–1256 (2008).
59. Maddison, W. P. & Maddison, D. R. Mesquite: a modular system for evolutionary analysis. v. 2.75. (2011); www.mesquiteproject.org
60. Pebesma, E. J. & Bivand, R. S. sp: classes and methods for spatial data. R package v. 0.9-44. (2016).
61. Schnute, J. T., Boers, N., Haigh, R. & Couture-Beil, A. PBSmapping: PBS Mapping 2.59. R package version. (2015); www.cran.r-project.org
62. Dunning, J. B. *Handbook of Avian Body Masses* (CRC, Boca Raton, Florida 1993).
63. Nevo, E., Beiles, A. & Ben-Shlomo, R. The evolutionary significance of genetic diversity: ecological, demographic and life history correlates. In *Evolutionary Dynamics of Genetic Diversity. Lecture Notes in Biomathematics* Vol. 53 (ed. Mani, G. S.) 13–213 (Springer, Berlin, Heidelberg, 1984).
64. Cole, C. T. Genetic variation in rare and common plants. *Annu. Rev. Ecol. Evol. Syst.* **34**, 213–237 (2003).
65. Leffler, E. M. et al. Revisiting an old riddle: what determines genetic diversity levels within species? *PLoS Biol.* **10**, e1001388 (2012).
66. White, E. P., Ernest, S. K. M., Kerkhoff, A. J. & Enquist, B. J. Relationships between body size and abundance in ecology. *Trends Ecol. Evol.* **22**, 323–330 (2007).
67. Schielzeth, H. Simple means to improve the interpretability of regression coefficients. *Methods Ecol. Evol.* **1**, 103–113 (2010).
68. Grafen, A. The phylogenetic regression. *Phil. Trans. R. Soc. Lond. B-Biol. Sci.* **326**, 119–157 (1989).
69. Pinheiro, J., Bates, D., DebRoy, S., Sarkar, D. & Team, R. C. nlme: Linear and nonlinear mixed effects models. R package v. 3.1-117. (2014); <http://CRAN.R-project.org/package=nlme>
70. Bartoń, K. MuMIn: multi-model inference. R package v. 1.5 (2013).
71. Martin, P. R., Montgomerie, R. & Lougheed, S. C. Color patterns of closely related bird species are more divergent at intermediate levels of breeding range sympatry. *Am. Nat.* **185**, 443–451 (2015).
72. Baudat, F. & de Massy, B. Regulating double-stranded DNA break repair towards crossover or non-crossover during mammalian meiosis. *Chromosome Res.* **15**, 565–577 (2007).
73. De Massy, B. Initiation of meiotic recombination: how and where? Conservation and specificities among eukaryotes. *Annu. Rev. Genet.* **47**, 563–599 (2013).
74. Ellegren, H. & Fridolfsson, A. K. Male-driven evolution of DNA sequences in birds. *Nat. Genet.* **17**, 182–184 (1997).
75. Axelsson, E., Smith, N., Sundstrom, H., Berlin, S. & Ellegren, H. Male-biased mutation rate and divergence in autosomal, Z-linked and W-linked introns of chicken and turkey. *Mol. Biol. Evol.* **21**, 1538–1547 (2004).
76. Smit, A. F., Hubley, R. & Green, P. RepeatMasker Open-3.0. (2010); <http://www.repeatmasker.org>
77. Warren, W. C. et al. The genome of a songbird. *Nature* **464**, 757–762 (2010).
78. Backstrom, N. et al. The recombination landscape of the zebra finch *Taeniopygia guttata* genome. *Genome Res.* **20**, 485–495 (2010).
79. Poelstra, J. W. et al. The genomic landscape underlying phenotypic integrity in the face of gene flow in crows. *Science* **344**, 1410–1414 (2014).
80. Dumont, B. L. & Payseur, B. A. Evolution of the genomic rate of recombination in mammals. *Evolution* **62**, 276–294 (2008).
81. Dumont, B. L. & Payseur, B. A. Evolution of the genomic recombination rate in Murid rodents. *Genetics* **187**, 643–657 (2011).
82. Smukowski, C. S. & Noor, M. A. F. Recombination rate variation in closely related species. *Heredity* **107**, 496–508 (2011).
83. Yu, G., Smith, D. K., Zhu, H., Guan, Y. & Lam, T. T. Y. ggtree: an R package for visualization and annotation of phylogenetic trees with their covariates and other associated data. *Methods Ecol. Evol.* **8**, 28–36 (2017).
84. Jenks, G. F. The data model concept in statistical mapping. *Int. Yearbook Cartogr.* **7**, 186–190 (1967).

Acknowledgements

We thank N. S. Bulatova, B. S. W. Chang, E. J. de Lucca, G. Semenov, P. Tang, I. M. Ventura, Y. Wu and the University of Chicago Library for their help in accessing cytological studies not available online; S. G. Dubay, K. Supriya and A. E. White for their assistance with statistical analyses and figure aesthetics; and A. Hipp, R. Hudson, M. Kronforst and M. Przeworski for their comments on the manuscript. Tissue materials for species without data on GenBank generously came from the Kansas University Biodiversity Institute and Natural History Museum (KU), the Field Museum of Natural History (FMNH) and the Australian National Wildlife Collection (ANWC). A. E. Johnson provided original artwork of the *Chloris* greenfinches used in Fig. 1.

Author contributions

D.M.H. collected the data, ran the analyses and wrote the manuscript, all with input from T.D.P. Supported in part by an NSF Doctoral Dissertation Improvement Grant (DDIG1601323) to T.D.P. and D.M.H.

Competing interests

The authors declare no competing financial interests.

Additional information

Supplementary information is available for this paper at doi:10.1038/s41559-017-0284-6.

Reprints and permissions information is available at www.nature.com/reprints.

Correspondence and requests for materials should be addressed to D.M.H.

Publisher's note: Springer Nature remains neutral with regard to jurisdictional claims in published maps and institutional affiliations.